The resistance of a $(Xe)_n$ atomic wire

L. Pizzagalli[1], C. Joachim[1], X. Bouju[2] and Ch. Girard[2]

[1] *Centre d'Élaboration de Matériaux et d'Études Structurales, UPR CNRS 8011*
29, rue Jeanne-Marvig, B.P. 4347, F-31055 Toulouse Cedex 4, France
[2] *Laboratoire de Physique Moléculaire, URA CNRS 772*
Université de Franche-Comté - F-25030 Besançon Cedex, France

Abstract. – The electrical resistances of different $(Xe)_n$ atomic wires are calculated. For Xe
and $(Xe)_2$, confined in the gap of a scanning tunneling microscope junction, the dynamics of
the xenon atoms upon approaching the probe tip is included. With a single Xe, in agreement
with the recent work of Yazdani *et al.* (*Science*, **272** (1996) 1921), a resistance of 0.06 MΩ
is found. The resistance of $(Xe)_2$ ranges between 10 MΩ and 30 MΩ due to both mechanical
deformations and electronic interferences. Finally, for longer $(Xe)_n$ wires, the resistance displays
an exponential behavior with respect to n and an inverse damping length of 0.74 Å^{-1}, very close
to that of an alkane chain, is predicted.

An atomic wire is an ordered chain of atoms that connects two metallic electrodes [1]-[3].
With a scanning tunneling microscope (STM) such linear structures can be assembled atom
by atom [4] or fabricated by extracting surface atoms one by one [5], [6]. The 1D character of
the chain leads to a relaxation of its structure with the opening of a gap at E_f (the metallic-
electrodes Fermi level) even if the chain interactions with the surface refrain it [6]. This gap
produces a nonlinear current-voltage (I-V) characteristic. To recover a linear regime, the bias
voltage has to be lower than the gap width [7] and a *tunneling transport regime* [7] (alternatively
called an off-resonant transport regime [8]) can be expected.

In a recent experiment, Eigler and co-workers have succeeded in assembling the shortest
members, Xe and $(Xe)_2$, of the $(Xe)_n$ atomic wire family, one Xe being adsorbed on the STM
tip apex and the other on the metal surface [8]. The resistance-distance (R-z_{tip}) characteristics
of the junction are recorded to track for an electric contact between the Xe-tip apex and the
surface Xe. This contact is defined by a saturation regime in the R-z_{tip} curve at small z_{tip} [8].
A resistance of 0.1 MΩ for Xe and of 10 MΩ for $(Xe)_2$ was measured and calculated. This
confirms the intuition that the resistance of a short Xe wire must increase with its length
similarly to what happens with a molecular wire on the long range [9].

The aim of this letter is threefold. First, we study the stabilization of both Xe and $(Xe)_2$
trapped by the tip of an STM. The range of tip-surface distances where $(Xe)_2$ remains aligned
is determined. Second, we show that the saturation of the junction resistance observed at
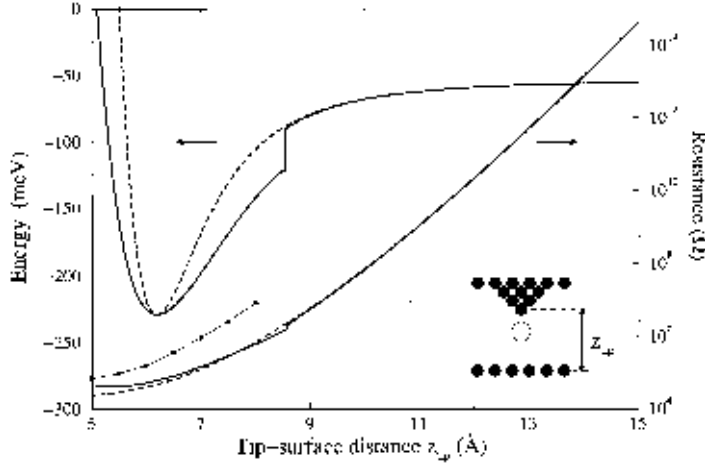
Fig. 1. – Variation of the Xe potential energy (upper left part) and of the Xe junction resistance (lower right part) *vs.* the tip-surface distance. The distance z_{tip} is defined from the least atom of the tip-apex to the first layer of the surface. For large tip-surface separations, the Xe atom is located at its equilibrium distance (3.43 Å) just beneath the tip apex. Full and dashed lines correspond to a free Xe atom and to a Xe atom frozen at its 3.43 Å equilibrium distance, respectively. The experimental data from ref. [8] are also reported (black dots).

small tip-sample distance does not correspond to the stabilization of a Xe wire under electrical contact conditions. Finally, we study the exponential increase of the $(Xe)_n$ wire resistance with respect to its length (where n varies from 1 to 10).

Let us consider an STM junction composed of a [111]-oriented copper tip facing a Cu(110) surface (see insets of figs. 1 and 2). When the tip is approached towards the surface, the positions of the two Xe in the junction (one being adsorbed on the surface and the other on the tip) verify the coupled equations of motion:

$$m_{Xe}\ddot{\mathbf{r}}_i(t) = -\boldsymbol{\nabla}[V_{as}(\mathbf{r}_i) + V_{at}(\mathbf{r}_i) + V_{aa}(\mathbf{r}_i - \mathbf{r}_j)] = \gamma\dot{\mathbf{r}}_i(t), \qquad (1)$$

where the indices i and j can take the values 1 or 2. $V_{as}(\mathbf{r})$ represents the interaction energy of a single Xe atom physisorbed on the Cu(110) surface. This contribution will be accounted for by a pairwise dipolar and quadrupolar extended Born-Mayer potential [10]. $V_{at}(\mathbf{r})$ describes the Xe atom interaction with the tip apex. A special care has been taken with the construction of this potential in order to include, simultaneously, many-body and anisotropic effects in the van der Waals binding between the Xe atom and the supported metallic apex [11]. In this dynamical study, $V_{at}(\mathbf{r})$ is calculated up to the N-body dipolar terms by using a generalized propagator technique [12]. For the $(Xe)_2$ case, an additional term V_{aa} described the Xe-Xe interaction [13] has to be included. Finally, in eq. (1), γ is a semi-classical friction coefficient accounting for the energy damping introduced by the surface phonons [14]. Equations (1) are solved by a standard Verlet algorithm.

The current through the tip apex-Xe-surface junction is calculated from our elastic-scattering quantum chemistry technique (STM-ESQC) [15]. The values of the $(Xe)_n$ resistance are simply obtained from the V/I ratio, V and I being measured far from the junction. From Landauer's formula [16], this macroscopic resistance is a measure, normalized in Ohmic unit, of the electronic transparence [17] of the $(Xe)_n$ chain.

In ESQC, a multichannel transfer matrix is built from the full-valence electronic structure of the tunneling junction (the tip apex + the adsorbates + the surface). An effective Hamiltonian
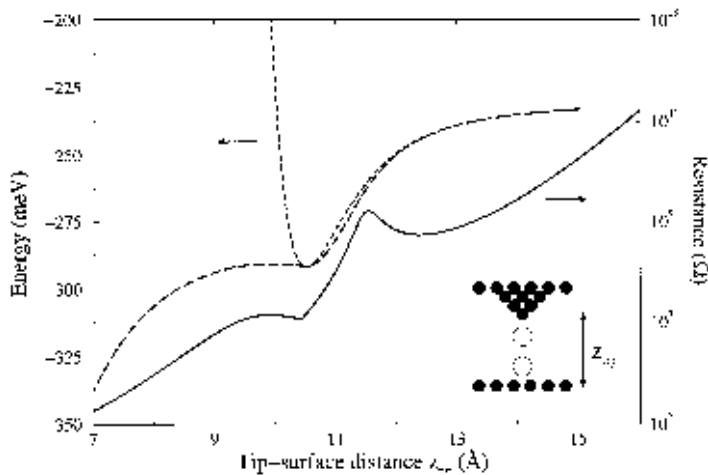
Fig. 2. – Variation of the total energy of the $(Xe)_2$ dimer (dashed and short-dashed lines) and the resistance (full line) as a function of tip-surface distance, for a tip-$(Xe)_2$-surface system. The dashed and full lines correspond to the free Xe atoms case. The short-dashed line represents the Xe atom energy sum when the two Xe are frozen, one located at 3.43 Å under the tip apex and the other located at 2.78 Å above the Cu(110) surface.

technique is used to couple this supermolecule to the bulk parts [15]. For each z_{tip} a time-averaged Xe position is calculated from eq. (1) and introduced in ESQC in an adiabatic approximation. The tip apex is a cluster of ten copper atoms [111] oriented. This cluster is supported by the (110) copper surface of the tip bulk. The other part of the junction is a Cu(110) slab surface. The Xe electronic structure is described by its filled $5p$ and empty $6s$ atomic orbitals as already optimized in [15]. The $5p$ orbitals are required to properly describe the $(Xe)_2$ molecular orbitals at small Xe-Xe distances when the two Xe atoms are constrained by the tip apex. To limit the computation time, each Cu atoms in the junction is restricted to its $4s$ orbital. Only the copper atom ending the tip is described by a double zeta basis set to recover a current variation of one order of magnitude per angström.

For a single xenon, three different regimes of mechanics can be defined in the junction.

i) Beyond a critical distance $z_{tip} > 8.55$ Å, the Xe is trapped by the tip apex and the resistance increases exponentially when the Xe-terminated tip is retracted (fig. 1). The tunneling process is non-resonant [8], [10].

ii) For 6.20 Å $\leq z_{tip} \leq 8.55$ Å, a competition occurs between the adsorption of the Xe on the apex and on the Cu(110) surface. The Xe leaves the tip for a surface adsorption site (fig. 1) because of the collapse of the tip potential well [10]. This change has a negligible impact on the junction resistance (fig. 1) since, in this z_{tip} range, the electronic-structure modification between a Xe adsorbed on the surface or trapped to the end tip remains weak. In this distance range, the mixing between Xe and Cu orbitals is not efficient enough to maximize I. Therefore, no electrical contact can be established in this case.

iii) For small distances ($z_{tip} < 6.20$ Å), the junction enters a repulsive regime for which the Xe orbitals overlap strongly with the metal ones. The resistance of the junction starts to saturate (fig. 1). This is the electrical contact regime with a junction resistance of about 0.06 MΩ, very close to the value found experimentally and calculated for the Ni(110)-Xe-W tip junction [8].
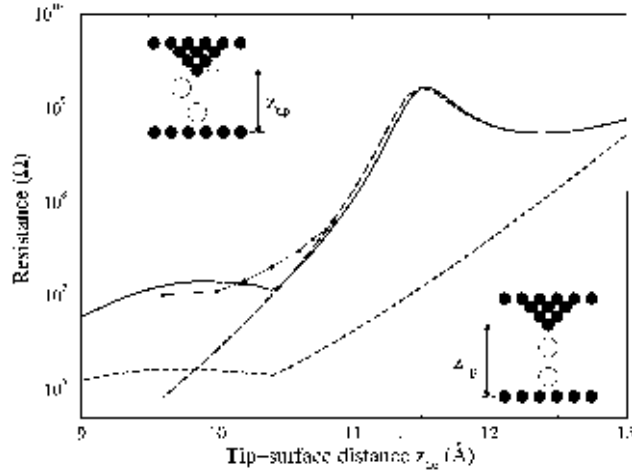
Fig. 3. – Variation of the junction resistance as a function of the tip-surface distance, for a tip-$(Xe)_2$-surface system and at a smaller $z_{\rm tip}$ range than in fig. 2. The full line shows the resistance for two free Xe. The dashed line represents the resistance with two frozen Xe and the short-dashed line the resistance when the Xe atoms are allowed to move during the tip approach by removing all Xe-Xe overlap effects. The experimental data from ref. [8] are also reported (black dots).

When $(Xe)_2$ is located in the junction, some additional effects complicate the determination of the resistance. First, $(Xe)_2$ is not stable under the tip constraint. At small $z_{\rm tip}$ the Xe adsorbed on the tip prefers to go sideways, limiting the range where the electrical contact can be expected. Simultaneously, when $z_{\rm tip}$ is reduced, the magnitude of the direct *through space tunneling current* becomes very close to the one passing through the $(Xe)_2$ molecular states. We will discuss in the following how the superposition of these two paths is destructive and prevents the application of an Ohm's law like argument to separate them. Three different regimes of junction resistance can be defined for $(Xe)_2$.

i) For $z_{\rm tip} > 13.0$ Å an exponential variation of R with $z_{\rm tip}$ is obtained (fig. 2). This is consistent with the exponential decay of the *through space overlap* between the Xe atomic orbitals. This is also observed for $z_{\rm tip} \leq 9.5$ Å and is a consequence of the deformation of the dimer structure (fig. 2): if during the approach, the Xe-tip and Xe-Cu(110) spacings are maintained at a constant value, the energy curve presents a strong repulsive regime for $z_{\rm tip} < 10.5$ Å (fig. 2). But if this is performed with a fully relaxed configuration, one Xe is pushed sideways at the starting of the repulsive regime (fig. 2). Consequently, when $z_{\rm tip} \leq 9.5$ Å, the Xe on the surface supports progressively the main part of the current and the R-$z_{\rm tip}$ characteristic behaves like in fig. 1.

ii) For 9.5 Å $\leq z_{\rm tip} \leq 10.5$ Å, the resistance starts to saturate as with the experimental data reported in fig. 3. But this saturation is not sufficient to claim that a pure electric contact had occurred because the wire is already deformed and the tunneling current is partially flowing through a single Xe atom. For example, when during the approach, the resistance is calculated with the two Xe atoms frozen in their equilibrium position, the resistance saturation disappears (fig. 3).

iii) For 10.5 Å $\leq z_{\rm tip} \leq 13$ Å, the $(Xe)_2$ wire is not yet deformed by the tip apex. Therefore, the peculiar R-$z_{\rm tip}$ characteristic in fig. 3 with a bump at $z_{\rm tip} = 11.5$ Å reveals a pure electronic effect. But in the z range considered, each Xe atomic orbital starts to overlap with both the Cu(110) surface and the tip apex orbitals. This creates additional non-resonant tunneling paths via the states of each Xe, their tails being broadened by overlapping with the electrodes.
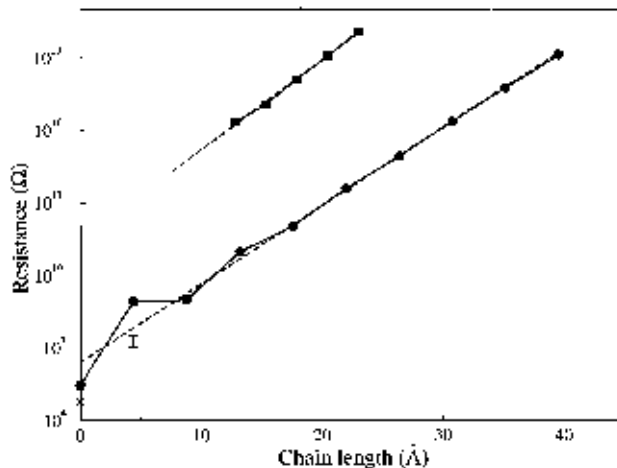
Fig. 4. – Variation of the resistance of a $(Xe)_n$ chain (filled circle) and an alkane chain $CH_3(CH_2)_n CH_3$ (filled square) as a function of their chain length L defined as the distance between the first and the last chain elements. These resistances were calculated by connecting each end of a chain to a flat Cu(110) surface and the dashed lines show the exponential fit of the $R(L)$ law. Our estimations for the Xe (cross) and $(Xe)_2$ (error bar) contacted by a tip apex are also reported.

At E_f, these will complement the non-resonant tunnel channels defined by the tails of the $(Xe)_2$ molecular states. But the electronic phase shift through the new channels is different from the one through the $(Xe)_2$ molecular-states channels. Therefore, the superposition of all these tunneling channels is not constructive, producing the R-bump for $z_{tip} = 11.5$ Å and the fast decrease observed experimentally for 10.5 Å $\leq z_{tip} \leq$ 11.5 Å. This is a beautiful example of interferences between non-resonant tunneling channels, resonating far from E_f. To get more insight into this point, we have calculated an R-z_{tip} characteristic by removing the overlap between the Xe atomic orbitals. In this case, the interferences are suppressed and a flat characteristic is obtained which does not fit the experimental data (fig. 3).

Furthermore, for 10.5 Å $< z_{tip} <$ 11.5 Å these interferences are the signature of the formation of the $(Xe)_n$ electronic band structure: there is a progressive decrease of the density of state in the gap between the highest occupied-lowest unoccupied electronic states of the $(Xe)_n$ chains when the Xe are added one by one to the chain. In the gap, without those interferences, the tails of the electronic states added by a new Xe would increase the density of states at E_f. An experimental study of the R-z_{tip} curve is a unique opportunity to observe continuously this phenomenon because, in the z_{tip} range considered, the Xe-Xe distance can be changed between 4.3 to 5.1 Å (the equilibrium Xe-Xe distance in the bulk being 4.4 Å [18]).

To determine the contact resistance on $(Xe)_2$, the R-z_{tip} characteristics are compared with the z-dependent internal mechanics of the junction (tip changes, adsorbate displacements) during the tip approach [17]. For $z_{tip} > 11.5$ Å, there is not enough mixing between the adsorbed surface Xe and the apex Xe orbitals to reach a large current I. This orbital mixing occurs for z_{tip} values lower than the distance where then van der Waals attractive interactions are equilibrated by Xe core-core repulsion. This is the case for 9.5 Å $\leq z_{tip} \leq$ 10.5 Å in the R-z_{tip} saturation regime. But due to the mechanical deformations, almost one Xe participates to this contact. In the intermediate z_{tip} range, where $(Xe)_2$ is not deformed, interferences are dominant and I is not maximized as required for an electrical contact. Therefore, we can only propose an estimation of the $(Xe)_2$ resistance, between 10 MΩ (the R-z_{tip} saturation resistance already calculated in [8]) and 30 MΩ (determined on the R-z_{tip} characteristic at 4.4 Å Xe-Xe

distance).

Extending the $(Xe)_n$ chain length further than $n \geq 2$, the wire resistance can be calculated with the ESQC technique, the Xe being maintained in a chain configuration between two Cu(110) pads at the known 4.4 Å equilibrium Xe-Xe distance. This is presented in fig. 4 up to $n = 10$. The resistance of the first member of the series $[(Xe)_2, (Xe)_3]$ does not line up on the $R = R_0 \exp[\beta L]$ fit of the $R(L)$ curve (fig. 4). This is due to the interference effects already discussed for $(Xe)_2$ and becomes negligible for $(Xe)_4$ due to the small overlap between the first and last Xe in the chain. From fig. 4, the inverse damping length is $\beta = 0.74$ Å^{-1} with the $5p$ and $6s$ atomic orbitals taken into account. The $R(L)$ exponential law (fig. 4) will lead to a tunneling transport regime through a large-gap wire, a $(Xe)_n$ having a filled empty-states gap of 9 eV. For comparison, the variation of an alkane chain resistance with length [9], [19] has been reported in fig. 4. The filled empty-states gap for an alkane chain stabilizes at 8.9 eV [20] giving $\beta = 0.85$ Å^{-1}. This shows that independently of the organic or inorganic character of a nanoscale wire, the same order of magnitude in the band gap leads to the same damping length.

In conclusion, the deformation of a Xe atomic wire upon approaching the contact STM electrode does not allow to define a precise contact resistance. The tunnel junction may be useful as a nanoscale sensor. When the structure of the wire is stabilized, the variation of the resistance *vs.* its length is exponential. This is independent of the organic or inorganic character of the wire. Finally due to its small damping length, a $(Xe)_n$ wire will not be the best candidate to make a nanoscale wire.

<p align="center">***</p>

REFERENCES

[1] JOACHIM C., BOUJU X. and GIRARD CH., in *Atomic and nanometer-scale modification of materials: fundamental and applications*, *NATO ASI Ser. E*, Vol. **242**, edited by PH. AVOURIS (Kluwer, Dordrecht) 1993, pp. 247-261.
[2] LANG N. D., *Phys. Rev. B*, **52** (1995) 5335.
[3] YAMADA T., YAMAMOTO Y. and HARRISON W. A., *J. Vac. Sci Technol. B*, **14** (1996) 1243.
[4] EIGLER D. M. and SCHWEIZER E. K., *Nature*, **344** (1990) 524.
[5] HOSAKA S. *et al.*, *J. Vac. Sci. Technol. B*, **13** (1995) 2813.
[6] WATANABE S. *et al.*, *Phys. Rev. B*, **52** (1995) 10768.
[7] JOACHIM C. and GIMZEWSKI J. K., *Europhys. Lett.*, **30** (1995) 409.
[8] YAZDANI A., EIGLER D. M. and LANG N. D., *Science*, **272** (1996) 1921.
[9] JOACHIM C. and VINUESA J. F., *Europhys. Lett.*, **33** (1996) 635.
[10] BOUJU X., JOACHIM C., GIRARD CH. and SAUTET P., *Phys. Rev. B*, **47** (1993) 7454.
[11] BOUJU X., GIRARD CH., PIZZAGALLI L. and JOACHIM C., in preparation (unpublished).
[12] GIRARD CH., MARTIN O. J. F. and DEREUX A., *Phys. Rev. Lett.*, **75** (1995) 3098.
[13] KOUTSELOS A. D., MASON E. A. and VIEHLAND L. A., *J. Chem. Phys.*, **93** (1990) 7125.
[14] PERSSON B. N. J., *Surf. Sci*, **269/270** (1992) 103.
[15] JOACHIM C., SAUTET P. and LAGIER P., *Europhys. Lett.*, **20** (1992) 697.
[16] LANDAUER R., *Z. Phys. B*, **68** (1987) 217.
[17] JOACHIM C., GIMZEWSKI J. K., SCHLITTLER R. R. and CHAVY C., *Phys. Rev. Lett.*, **74** (1995) 2102.
[18] KITTEL C., *Introduction to Solid State Physics* (John Wiley and Sons, New York) 1976.
[19] SALMERON M. *et al.*, *Langmuir*, **9** (1993) 3600.
[20] DEWAR M. J. S., YAMAGUCHI Y. and SUCK S. H., *Chem. Phys.*, **43** (1979) 1451.